

Original Article

Applied research on confocal microscopy through focusing detection of tarsal glands shape following phacoemulsification for cataract

Mengke Yuan¹, Qin Zhang^{2*}, Libin Chang¹

¹Department of Ophthalmology, Beijing Yanhua Hospital, Beijing 102500, China; ²Department of Ophthalmology, Peking University People's Hospital, Beijing 102500, China. *Equal contributors.

Received February 12, 2021; Accepted April 12, 2021; Epub September 15, 2021; Published September 30, 2021

Abstract: Objective: To investigate the value of confocal microscopy in determining the morphology of the tarsal gland after cataract phacoemulsification. Methods: A total of 74 patients (74 eyes) who underwent phacoemulsification for a monocular cataract and intraocular lens implantation (all were single eye surgeries) in our hospital from May 2018 to October 2018 were recruited as the study cohort, with 43 male patients and 31 female patients, and a mean age of (64.8±12.5) years old. All the patients were followed up for 6 months, of whom 25 cases with MGD were included in the MGD group and 49 cases without MGD were included in the control group. All the patients were examined within 30 days and underwent IVCM inspections of the acinar morphology of the tarsal glands (expansion and atrophy), the infiltration of the inflammatory cells in the tarsal gland tissue, and a classification of the fibrosis in the tarsal gland tissue. Results: The longest and shortest acinar diameters in the MGD patients were significantly greater than they were in the control group, but the acinar areas were smaller than they were in the control group. The meibomian glandular vesicle densities, the average opening diameters, the fibrosis, and the inflammatory cell density in the MGD group were significantly increased. Conclusion: IVCM plays a vital role in the early diagnosis, in the severity grading, and in the evaluation of the clinical effectiveness of MGD-related diseases, by which the morphological changes of the tarsal gland after phacoemulsification can be observed in a timely manner to predict the occurrence of MGD.

Keywords: IVCM, cataracts, meibomian glands, morphology

Introduction

Cataract phacoemulsification is by far the most advanced cataract procedure. It has many advantages, such as minor tissue injury and a quick postoperative recovery. In spite of the satisfactory recovery from hyperopia, patients normally experience postoperative ocular surface discomfort, poor myopia, and decreased contrast sensitivity. Prior trials pointed out that these symptoms may be associated with tarsal gland dysfunction, and most of them were caused by eye drops, decreased corneal sensitivity, and the loss of conjunctival goblet cells [1, 2].

Meibomian gland dysfunction (MGD) is the most common cause of dry eye over-evaporation. It is characterized by chronic and diffuse tarsal gland abnormalities, the obstruction of the terminal duct in the tarsal gland, and

changes in the quality and quantity of the tarsal gland secretions [3]. In vivo confocal microscopy (IVCM), a non-invasive ophthalmic imaging diagnostic technique, can provide high resolution images at the cellular level to show the structural features of the ocular surface tissue, so clinicians can respond to the characteristics of the tarsal gland in advance [4]. Therefore, determining how to use IVCM to evaluate whether cataract surgery will affect the tarsal gland function and to predict the occurrence of MGD may have some value in guiding clinical practice.

Materials and methods

General data

A total of 74 patients (74 eyes) who underwent phacoemulsification for monocular cataracts and intraocular lens implantations (all were

single eye surgeries) in our hospital from May 2018 to October 2018 were recruited as the study cohort, with 43 male patients and 31 female patients, and a mean age of (64.8±12.5) years old. The protocol was approved by Peking University First Hospital Biomedical Research Ethics Committee with approval number 2018 (438)-83. Inclusion criteria: (1) Patients 50 to 80 years old, (2) Patients with an age-related cataract and with a best-corrected visual acuity ≤ 0.5 , and with non-obstructive MGD before the operation. (3) Written informed consent was obtained from all the participants. Exclusion criteria: (1) Patients with other eye diseases such as allergic ocular surface diseases, or a preoperative history of continuous ocular local administration, or a history of ocular surgery or trauma. (2) Patients also suffering from eyelid inflammation, such as hordeolum external, chalazion, or blepharitis. (3) Patients with congenital tarsal gland structure abnormalities, such as congenital ectodermal dysplasia or congenital aniridia syndrome. (4) Patients who also have severe obstructive MGD: a palpebral margin morphological score > 3 positive signs, or whose lipids of the tarsal gland secretion are reduced (> level 2). (5) Patients with severe liver or kidney dysfunction or other serious systemic diseases.

All the patients were followed up for 6 months after the operations, and the patients who met the MGD diagnostic criteria were included in the MGD group, and the rest were placed in the control group. The MGD diagnostic criteria according to the *Recommendations of the International Symposium on Tarsal Gland Dysfunction (2011)* [5], include conscious symptoms of ocular surface discomfort, such as a burning sensation, itchy eyes, dry acerbity, visual fluctuations, eye red, etc., and tarsal gland defects, such as abnormal tarsal margins and opening, changes in the quantity and quality of tarsal gland secretions (including changes in the blepharolipid traits and difficulty in elimination). At least one of these signs is considered MGD.

IVCM inspection

We used the “RCM module” in the IVCM to observe the structure of the tarsal glands (HRT-3, Heidelberg Engineering Corporation,

Germany). Machine parameters: The laser wavelength is 670 nm, the observation of the visual field is 400 μm \times 400 μm , the image resolution is 384 pixels \times 384 pixels, the magnification is 800 times, and the axial resolution is 1 μm . All the patients were examined within 30 days after their IVCM operations [6].

Methods of inspection: surface anesthesia (0.5% propamecaine) of the eye was performed before the examination, lubricating carbomer eye gel was applied to the IVCM lens surface (Bausch and Lomb Corporation, Germany), and disposable corneal contact caps (Tomo-Cap, Heidelberg Engineering Corporation, Germany) were installed.

The forehead and mandible were fixed for the examinations, and the patients were asked to look up, open the lower eyelid of the examined eye and to fully expose the tarsal gland of lower eyelid. The IVCM lenses were advanced to contact the lower eyelid conjunctiva to start scanning. The scans were performed from the palpebral margin to the temporal side of the nose, and the parallel scans were performed until the entire tarsal gland scan was completed [7, 8]. In this study, the morphological parameters of the right lower eyelid tarsal gland were statistically analyzed.

Outcome measures

The acinar morphology of the tarsal gland (including any expansion or atrophy), the infiltration of the inflammatory cells in the tarsal gland tissue, and the classification of the fibrosis in the tarsal gland tissues were observed. The acinar morphology of the tarsal gland was evaluated as follows: Three random images of the IVCM of the tarsal gland that form the inferior eyelid conjunctiva nasal, the central and temporal three longitudinal parts, and the opening of the tarsal gland, near the margin of the eyelid, near the vault of the three transverse parts of the intersection were selected. A semi-automatic analysis was conducted using Image J software, including the meibomian gland acinar longest diameter (MGALD), the meibomian gland acinar shortest diameter (MGASD), the meibomian gland acinar unit density (MGAUD), and the meibomian gland acinar unit area (MGAUA). “Area value” is the pixel value, which needs to be converted

Table 1. Comparison of general data between the two groups [n (%), ($\bar{x} \pm s$)]

group	n	male patients	female patients	Average age (years)	MGD Family history
MGD	25	13 (52.00)	12 (48.00)	63.14±12.72	5 (20.00)
control	49	30 (61.22)	19 (38.78)	65.28±12.21	7 (14.29)
χ^2/t			0.579	0.703	0.088
P			0.447	0.484	0.766

Table 2. Comparison of the parameters of the lower IVCM acinar of the tarsal gland

group	n	Acinar diameter (μm)		acinar density (/mm ²)	openings diameter (μm)
		max	min		
MGD	25	126.80±36.10	34.25±10.27	59.74±17.82	26.31±5.74
control	49	64.83±10.17	23.15±5.47	94.13±21.62	20.82±5.03
t		11.241	6.084	6.942	4.233
P		<0.001	<0.001	<0.001	<0.001

using the following formula: Actual area = area $\times 400 \times 400 / (384 \times 384) \mu\text{m}^2$.

Inflammatory cell infiltration in tarsal gland tissue: The density of the meibomian adenitis cells was measured using HRT-3 cell counting software for the IVCM images at the above 9 points, and the inflammatory cell density <300 mm² was reported in the healthy people [9]. Tarsal gland fibrosis grades: the IVCM images of the above nine points were observed; level 0 indicates normal eyelid conjunctival epithelial cells, with no fibrosis; level 1 indicates no more than half the extent has fibrosis; level 2 indicates more than half the extent has fibrosis [8].

About 5 mL of venous blood was taken from the subjects on an empty stomach, centrifuged, and isolated; the IL-1 β (Catalog # PDLB50), IL-6 (Catalog # PD6050), TNF- α (Catalog # PDTA00D), and hs-CRP (Catalog # PDCRP00) levels were measured using ELISA. All the Elisa kits were provided by R&D Systems.

Statistical analysis

The data analysis was done using SPSS 23.0. The quantitative data consistent with a normal distribution were expressed as ($\bar{x} \pm s$) and analyzed using t tests. The qualitative data were expressed as n (%) and analyzed using χ^2 tests. When the theoretical frequency <5, chi-square

tests were used. The grade data were analyzed using rank sum tests. Significance was declared at $P < 0.05$.

Results

Comparison of the general data

A total of 74 patients (74 eyes) were enrolled. The MGD group included 13 male and 12 female, with a mean age of (63.1±12.7) years old. The control group included 30 male and 19 female, with a mean age of (65.2±12.2) years old. The baseline data of the two groups were homogeneous (**Table 1**).

Comparison of the parameters of the lower IVCM acinar of tarsal gland

The acinar dilation of the tarsal gland near the palpebral margin, the diameter of the acinar increased significantly, the maximum diameter of the acinar was (126.80±36.10) μm and the min diameter of acinar (34.25±10.27) μm , and these values were all significantly higher in the MGD group than they were in the control group [(64.83±10.17) μm , (23.15±5.47) μm]. And the acinar density (59.74±17.82) was significantly reduced in the MGD patients, as compared to the control group (94.13±21.62)/mm². The average diameter of the glandular opening of the eyelid plate (26.31±5.74) μm was remarkably greater in the MGD patients compared to the control group (20.82±5.03) (**Table 2** and **Figure 1**).

Comparison of the parameters of the IVCM pathological results of the tarsal gland

After the phacoemulsification of the cataracts, the MGD patients had higher fibrosis levels (1.54±0.51), when compared to the control group (0.48±0.13). At the same time, the MGD patients showed smaller adenoid areas of dry eye symptoms (746.59±180.32) μm^2 compared to the control group (987.16±179.33) μm^2 ; A higher inflammatory cell density (352.94±101.56)/mm² was observed in the MGD patients compared to the control group

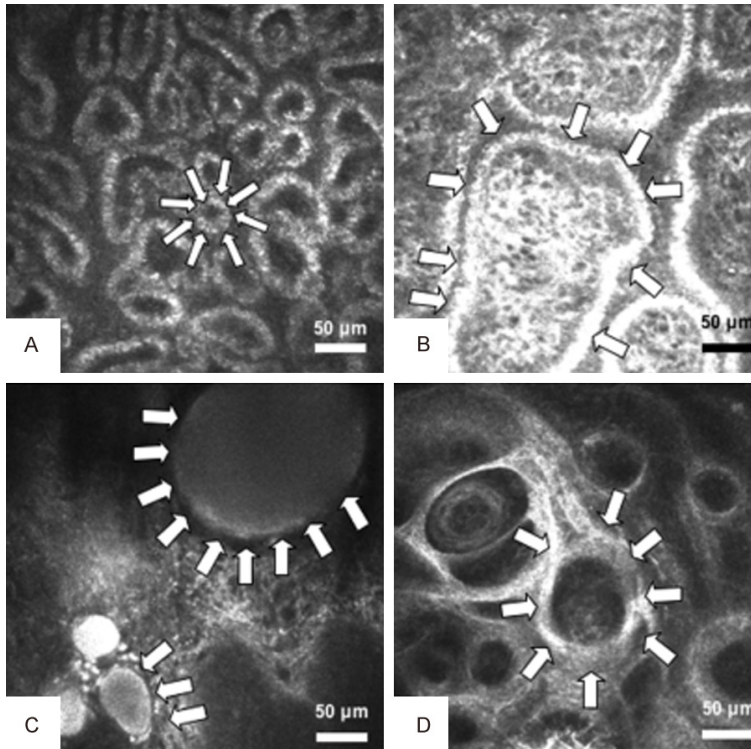


Figure 1. Comparison of the parameters of lower IVCM acinar of tarsal gland. A and B. Bleb density of the control group, a large number of dense acinar can be seen. C and D. MGD patients' acinar density, acinar atrophy and periglandular fibrosis can be seen.

Table 3. Comparison of the parameters of the IVCM pathological results of the tarsal gland

group	n	fibrosis level	adenoid area of dry eye symptom (μm^2)	inflammatory cell density (/mm ²)
MGD	25	1.54±0.51	746.59±180.32	352.94±101.56
control	49	0.48±0.13	987.16±179.33	174.82±83.17
Z		13.781	5.448	8.077
P		<0.001	<0.001	<0.001

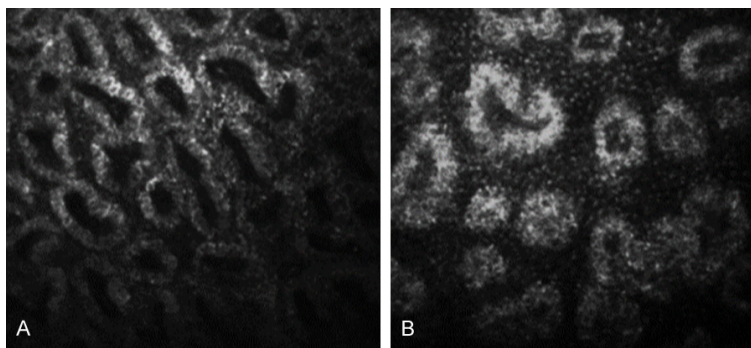


Figure 2. Comparison of the parameters of the inflammatory cells in the IVCM of the palpebral gland. A. Infiltration of the inflammatory cells in the control group. B. Infiltration of the inflammatory cells in the MGD group.

(174.82±83.17) (Table 3 and Figure 2). The number of people in grades 0, 1, 2 among the MGD patients and the control group were 0, 11, 14 vs 20, 29, 0) (Table 4).

Comparison of the inflammatory factors

Higher TNF- α , IL-1 β , IL-6, and hs-CRP levels were identified in the MGD patients, suggesting that there was a significant inflammatory response in the MGD patients (Table 5).

Discussion

The tarsal gland, perpendicular to the tarsal margin, is the body's largest sebaceous gland, distributed in the upper and lower eyelid lamellar layers, with 30-40 percent in the upper eyelid layer, and 20-30 percent in the lower eyelid layer. The histological structures of the glands of the eyelid plate include the acinar and the ducts, and these structures can synthesize, store, and secrete the lipid layer that forms the tear film, which plays an important role in maintaining tear film stability and preventing tear evaporation [9]. MGD is a chronic, diffuse meibomian gland disorder, usually characterized by the obstruction of the terminal duct of the tarsal gland or by changes in the amount of the secretions of the tarsal gland, which can lead to changes in the tear film, eye irritation, inflammation, and ocular surface disease [10]. In recent years, the number of phacoemulsification patients has been on the rise yearly. Extensive findings show that some patients experience MGD after cataract operations, resulting in corneal dryness and corneal epithelial

Table 4. Distribution of the two groups with different levels of fibrosis

group	n	Level 0	Level 1	Level 2
MGD	25	0 (0.00)	11 (44.00)	14 (56.00)
control	49	20 (40.82)	29 (59.18)	0 (0.00)
Z			-5.732	
P			<0.001	

Table 5. Comparison of the two groups' inflammatory factors

group	n	TNF- α (ng/l)	IL-1 β (ng/ml)	IL-6 (ng/ml)	hs-CRP (μ g/ml)
MGD	25	26.51 \pm 5.28	64.72 \pm 11.73	59.77 \pm 13.21	3.16 \pm 0.62
control	49	13.74 \pm 3.15	26.83 \pm 6.94	31.25 \pm 8.09	1.29 \pm 0.27
t		13.032	17.461	11.503	18.101
P		<0.001	<0.001	<0.001	<0.001

defects, which in turn can affect the visual acuity of patients in severe cases, and undermine the effect of the surgical treatment. Therefore, determining how to predict the occurrence of MGD in cataract phacoemulsification is of paramount importance.

Currently, clinical observation mainly through the palpebral margin, infrared tarsal gland photography, TBUT determination, and fluorescein staining are used for clinical observation in the corneal conjunctiva to diagnose MGD. Although these methods are highly specific and sensitive, all of them are an indirect evaluation. Tarsal glandography, an important diagnostic index of diagnostic MGD, can observe the structure, movement, distribution and absence of the tarsal gland in morphology, yet it can only be used to quantitatively analyze the loss rate of the tarsal gland, and cannot show the pathological, physiological, or inflammatory processes of the meibomian gland at the cellular level, and it is also difficult to observe the morphological characteristics of the tarsal acinar [11]. Recently, the IVCN technique has been widely used in the diagnosis of ocular surface diseases, since it can observe and evaluate the inflammatory response, tissue damage, and the nerve distribution of the ocular surface at the living level [12]. Ortiz-Gomariz et al. [13] used IVCN to observe the structural characteristics of tarsal conjunctiva and lower tarsal gland in four healthy patients in 2005. Subsequently, some international scholars used IVCN to observe the morphological changes in the tarsal gland in MGD patients, healthy

people, keratoconjunctivitis patients, corneal contact lens patients, chronic graft-versus-host disease secondary dry eye patients, and primary Sjogren's syndrome patients. A number of studies have found that the diameter and density of MGD acinar, the density of the inflammatory cells between the acinar and the degree of fibrosis were significantly different from those of the healthy control population [14]. MGD patients' widths of the gland openings of the eyelid plate, their keratinization levels, and the distributions

of their acinar dilation and atrophy, are conducive to the exploration of MGD pathogenesis and influencing factors and provide the basis for evaluating and monitoring the therapeutic effect of MGD from the level of cell morphology [15].

Photographic findings showed that the morphology and pathological process of the tarsal gland acinar in the different regions were inconsistent, so we added the IVCN examination and analysis of the tarsal gland division at the margin of the eyelid and the near fornix [16]. The findings [17] by McCann et al. showed that the lower palpebral gland loss grade is greater than the upper eyelid, and the sensitivity was greater than the upper eyelid. Thus this study used IVCN to observe the morphological changes of lower eyelid blepharoptosis. Under the IVCN, the MGD group with the acinar near the palpebral margin showed irregular expansion, and the cubic cell structures around acinar disappeared. At the IVCN, the missing part of the gland in the eyelid plate glandography may show a large amount of fibrous tissue hyperplasia and inflammatory cell infiltration, but it cannot show the structures of the tarsal glandular acinar. According to human tarsal gland anatomy and animal MGD models, catheter hyperkeratosis and abnormal secretions (including increased secretions and changes in composition), changes in the lipid composition can elevate the melting point, resulting in increased secretion viscosity and further concentration and solidification [18]. Excessive keratinizing substances and coagulated secretions accu-

mulating in glandular ducts can cause acinar opening obstructions and acinar cystic dilatation, and the pressure on the acinar from the accumulating secretions also increases, and then compresses the acinus causing shrinkage [19]. The pressure on the proximal acinar is greater than that of the distal acinar with the accumulation of keratinized abscission and denatured secretions in the glandular ducts, the proximal acinar becomes atrophic with fibrosis, and the distant acinar shows irregular cystic dilatation. Distant acinar dilatation may be due to the obstruction of the acinar openings, compensatory dilatation, or the presence of both factors. A small number of severe cases of distal acinar may also develop into atrophy [20]. Also, we found that the diameters and areas of the distal acinar of the control group were also larger than the diameters and areas of the proximal acinar, and there was no significant irregular expansion, atrophy, or fibrosis of the acinar. A large amount of inflammatory cell infiltration can be seen in the tarsal gland, and massive mature dendritic cells were seen around the partially atrophic acinar; Moreover, the pseudopodia of the dendritic cells can be clearly observed and can be used to diagnose differential inflammatory obstructive MGD and non-inflammatory MGD [21].

Surface anesthesia and contact with the cap is needed when IVCM is conducted, and it can cause reactive tears and lead eyelid to slip, and have an impact on the location of the inspection. In addition, for lower eyelid skin elasticity and less eye fissure subjects, it's difficult to scan the entire lower tarsal gland, and a second physician to fix the lower eyelid may be needed [22].

Although this research has garnered remarkable results, there still exist some shortcomings. This study confirms the application value of confocal microscopes, but many hospitals are not yet equipped with confocal microscopes, so it may be restricted due to multiple inspection steps and its time-consuming nature.

Conclusion

MGD patients' widths of the gland openings of the eyelid plates, their degrees of keratinization, and their distributions of acinar dilations and atrophy are conducive to the exploration

of MGD pathogenesis and the influencing factors and provide the basis for evaluating and monitoring the therapeutic effect of MGD from the level of cell morphology. IVCM is of great significance to the early diagnosis of MGD related diseases, and it can detect morphological changes of the palpebral gland soon after cataract phacoemulsification, and can predict the occurrence of MGD.

Disclosure of conflict of interest

None.

Address correspondence to: Libin Chang, Department of Ophthalmology, Peking University People's Hospital, No. 15, Yingfeng Street, Yanshan, Fangshan District, Beijing 102500, China. Tel: +86-13488690344; E-mail: changlibin555@163.com

References

- [1] Sharma N, Singhal D, Nair SP, Sahay P, Sreesankar SS and Maharana PK. Corneal edema after phacoemulsification. *Indian J Ophthalmol* 2017; 65: 1381-1389.
- [2] Khurana S, Gupta PC, R B, Sharma VK and Ram J. Epithelial ingrowth post phacoemulsification in a case of recurrent pterygium. *Cornea* 2020; 39: 129-131.
- [3] Patel SV and McLaren JW. In vivo confocal microscopy of Fuchs endothelial dystrophy before and after endothelial keratoplasty. *JAMA Ophthalmol* 2013; 131: 611-8.
- [4] Mencucci R, Cennamo M, Favuzza E, Rechichi M and Rizzo S. Triphasic polymeric corneal coating gel versus a balanced salt solution irrigation during cataract surgery: a postoperative anterior segment optical coherence tomography analysis and confocal microscopy evaluation. *J Cataract Refract Surg* 2019; 45: 1148-1155.
- [5] Jaber RM, Harrod M and Goshe JM. Spontaneous regression of epithelial downgrowth from clear corneal phacoemulsification wound. *Am J Ophthalmol Case Rep* 2018; 10: 159-162.
- [6] Mencucci R, De Vitto C, Cennamo M, Vignapiano R, Buzzi M and Favuzza E. Femtosecond laser-assisted cataract surgery in eyes with shallow anterior chamber depth: comparison with conventional phacoemulsification. *J Cataract Refract Surg* 2020; 46: 1604-1610.
- [7] Balestrazzi A, Martone G, Pichierrri P, Tosi GM and Caporossi A. Corneal invasion of ocular surface squamous neoplasia after clear corneal phacoemulsification: in vivo confocal microscopy analysis. *J Cataract Refract Surg* 2008; 34: 1038-43.

Applied research on confocal microscopy following phacoemulsification

- [8] van Kooten TG, Koopmans SA, Terwee T, Langer S, Stachs O and Guthoff RF. Long-term prevention of capsular opacification after lens-refilling surgery in a rabbit model. *Acta Ophthalmol* 2019; 97: e860-e870.
- [9] Mastropasqua L, Toto L, D'Ugo E, Lanzini M, Mattei PA, Falconio G, Doronzo E, Diomedea F and Trubiani O. In vivo and in vitro results of an automated preloaded delivery system for IOL implantation in cataract surgery. *Int Ophthalmol* 2020; 40: 125-134.
- [10] Sükösd AK, Szabadfi K, Szabó-Meleg E, Gáspár B, Stodulka P, Sétáló G Jr, Gábrriel R, Nyitrai M, Biró Z and Ábrahám H. Surgical stress and cytoskeletal changes in lens epithelial cells following manual and femtosecond laser-assisted capsulotomy. *Int J Ophthalmol* 2020; 13: 927-934.
- [11] Mencucci R, Favuzza E, Scali G, Vignapiano R and Cennamo M. Protecting the ocular surface at the time of cataract surgery: intracameral mydriatic and anaesthetic combination versus a standard topical protocol. *Ophthalmol Ther* 2020; 9: 1055-1067.
- [12] Yang Y, Peng M, Duan Y, Huang X, Li K and Lin D. Opacification of a hydrophilic acrylic intraocular lens. *J Coll Physicians Surg Pak* 2017; 27: S58-S60.
- [13] Ortiz-Gomariz A, Higuera-Esteban A, Gutiérrez-Ortega ÁR, González-Méijome JM, Arance-Gil A and Villa-Collar C. Late-onset candida keratitis after Descemet stripping automated endothelial keratoplasty: clinical and confocal microscopic report. *Eur J Ophthalmol* 2011; 21: 498-502.
- [14] Babu K, Narasimha Murthy K and Ramachandra Murthy K. Wavelike epitheliopathy after phacoemulsification: role of in vivo confocal microscopy. *Cornea* 2007; 26: 747-8.
- [15] Patel DV, Phang KL, Grupcheva CN, Best SJ and McGhee CN. Surgical detachment of Descemet's membrane and endothelium imaged over time by in vivo confocal microscopy. *Clin Exp Ophthalmol* 2004; 32: 539-42.
- [16] Misra SL, Goh YW, Patel DV, Riley AF and McGhee CN. Corneal microstructural changes in nerve fiber, endothelial and epithelial density after cataract surgery in patients with diabetes mellitus. *Cornea* 2015; 34: 177-81.
- [17] Chang A, Fridberg A and Kugelberg M. Comparison of phacoemulsification cataract surgery with low versus standard fluidic settings and the impact on postoperative parameters. *Eur J Ophthalmol* 2017; 27: 39-44.
- [18] Zheng T, Yang J, Xu J, He W and Lu Y. Near-term analysis of corneal epithelial thickness after cataract surgery and its correlation with epithelial cell changes and visual acuity. *J Cataract Refract Surg* 2016; 42: 420-6.
- [19] Du X, Zhao G, Wang Q, Yang X, Gao A, Lin J, Wang Q and Xu Q. Preliminary study of the association between corneal histocytological changes and surgically induced astigmatism after phacoemulsification. *BMC Ophthalmol* 2014; 14: 134.
- [20] Watson SL, Abiad G and Coroneo MT. Spontaneous resolution of corneal oedema following Descemet's detachment. *Clin Exp Ophthalmol* 2006; 34: 797-9.
- [21] Borkar DS, Veldman P and Colby KA. Treatment of fuchs endothelial dystrophy by descemet stripping without endothelial keratoplasty. *Cornea* 2016; 35: 1267-73.
- [22] Liang H, Randon M, Michee S, Tahiri R, Labbe A and Baudouin C. In vivo confocal microscopy evaluation of ocular and cutaneous alterations in patients with rosacea. *Br J Ophthalmol* 2017; 101: 268-274.